NMR Spectroscopy

Deutsche Ausgabe: DOI: 10.1002/ange.201607535
Internationale Ausgabe: DOI: 10.1002/anie.201607535

Difference between Extra- and Intracellular T_1 Values of Carboxylic Acids Affects the Quantitative Analysis of Cellular Kinetics by Hyperpolarized NMR

*Magnus Karlsson, Pernille Rose Jensen, Jan Henrik Ardenkjær-Larsen, and Mathilde H. Lerche**

Abstract: *Incomplete knowledge of the longitudinal relaxation time constant (T_1) leads to incorrect assumptions in quantitative kinetic models of cellular systems, studied by hyperpolarized real-time NMR. Using an assay that measures the intracellular signal of small carboxylic acids in living cells, the intracellular T_1 of the carboxylic acid moiety of acetate, ketoisocaproate, pyruvate, and butyrate was determined. The intracellular T_1 is shown to be up to four-fold shorter than the extracellular T_1. Such a large difference in T_1 values between the inside and the outside of the cell has significant influence on the quantification of intracellular metabolic activity. It is expected that the significantly shorter T_1 value of the carboxylic moieties inside cells is a result of macromolecular crowding. An artificial cytosol has been prepared and applied to predict the T_1 of other carboxylic acids. We demonstrate the value of this prediction tool.*

Biology is governed by dynamic changes across multiple distance- and time-scales. In turn, an impressive number of biological activities execute and respond to such dynamic changes in a highly organized and intricately regulated manner. To study such activities in a meaningful context, we require methods that allow us to directly assess functional characteristics in the physiological environments.[1] NMR spectroscopy is a non-disruptive and quantitative analytical tool, in which NMR signal intensities reflect the absolute concentrations of molecules. Time-dependent changes of these signals provide quantitative information about the processes acting on NMR-visible components. The underlying rationale of real-time NMR approaches for monitoring metabolic processes is to detect the chemical conversions of supplied isotope-labeled compounds through changes of their spectral properties and the NMR signatures of their transformation.[2] While sensitivity remains a challenge for conventional NMR spectroscopy, real-time NMR using dissolution dynamic nuclear polarization (dDNP) is particularly well-suited for metabolic studies.[3] With this technique, the utility of NMR is broadened by an increase of sensitivity of many orders of magnitude obtained by ex situ hyperpolarization. While individual NMR signatures of chemical entities (CE) are readily obtained, the measured signals are, however, functions of the CE concentration and a CE specific relaxation time constant that is dependent on the chemical and physical environment in which the CE is measured. If this relaxation time constant (spin lattice, T_1) is known, real-time NMR using dDNP is a strong method for the in situ quantification of metabolic reactions with complex kinetics. Herein, we measure the intracellular T_1 of small carboxylic acids in living cells and demonstrate an experimental prediction tool for the intracellular T_1 that allows the data fitting of complex kinetics.

A cellular system for the simultaneous detection of intra- and extracellular CE acted as a basis for data modeling of the intracellular T_1.[4] (Supporting Information, Section S1). Hyperpolarized [1-^{13}C]acetic acid was supplied to a suspension of living yeast cells at pH 4.2. The intracellular component, acetate at pH 6.1, as well as the extracellular component, acetic acid at pH 4.2, were measured over 2 min with a repetition time of 0.7 s (Figure 1). Because the chemical shift is sensitive to pH, a simple titration of acetate allows the determination of the intracellular pH (Supporting Information, Section S2). No active cellular transportation of acetic acid takes place in glucose-fed yeasts.[5] In such cells, undissociated acetic acid crosses the plasma membrane by diffusion.[6] At an extracellular pH of 4.2, well below the pKa of acetic acid (4.76), 78% of acetic acid is protonated and available for diffusion into the yeast cells. An intracellular pH of approximately 6.1 is maintained throughout the experiment, which leads to dissociation and effective trapping of acetate in the intracellular compartment (Figure 1A). The evolution of intra- and extracellular signals was fitted to a two-pool model, which resulted in the unambiguous determination of the intracellular T_1 of [1-^{13}C]acetate, with a value of 9 ± 1 s (Figure 1B,C). The value obtained for the intracellular T_1 could be verified in an experiment in which a paramagnetic agent quenched the extracellular acetic acid signal. A solution of the gadolinium complex Gd-DO3A was supplied to the yeast-cell suspension 15 s after the addition of hyperpolarized acetic acid. This paramagnetic complex quenches the hyperpolarization of the extracellular acetic acid signal by coordination and rapid exchange, while leaving the intracellular signal intact (Figure 1D).[7] Both methods yielded values for the intracellular T_1 of acetate of approx-

[*] Dr. M. Karlsson, Dr. P. R. Jensen, Prof. J. H. Ardenkjær-Larsen, Dr. M. H. Lerche
Technical University of Denmark, Department of Electrical Engineering, Center for Hyperpolarization in Magnetic Resonance
Building 349, DK-2800 Kgs Lyngby (Denmark)
E-mail: mhauler@elektro.dtu.dk
Homepage: www.dnp.dtu.dk
Supporting information and the ORCID identification number(s) for the author(s) of this article can be found under: http://dx.doi.org/10.1002/anie.201607535.

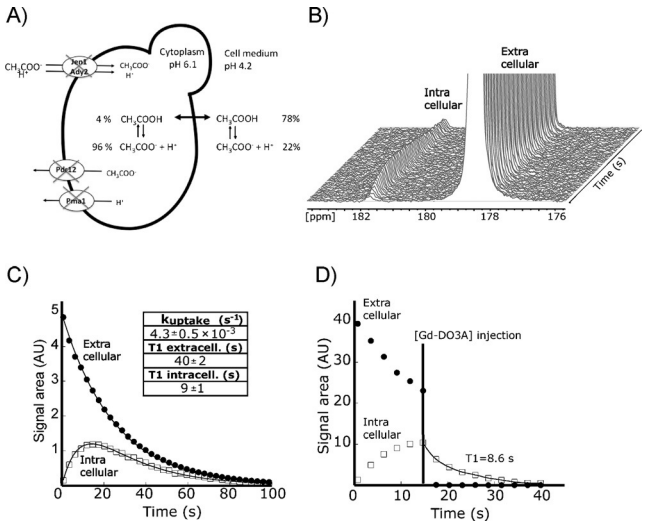

Figure 1. A) Experimental setup and overview of known transporters of small carboxylic acids in yeast.[5] B) Extracellular (178.4 ppm) and intracellular (181.8 ppm) signal evolution. C) Fitting of the model is shown for one dataset (2 mM). Signals in (C) are modeled using a two-pool model including four datasets (0.5 mM and 2 mM, $n=4$). The inset table lists measured average uptake rates and T_1 relaxation constants. D) Evolution of intracellular and extracellular acetate signal after addition of Gd-DO3A. T_1 of intracellular acetate is in this experiment measured as the exponential decay of acetate with a value of 8.6 s.

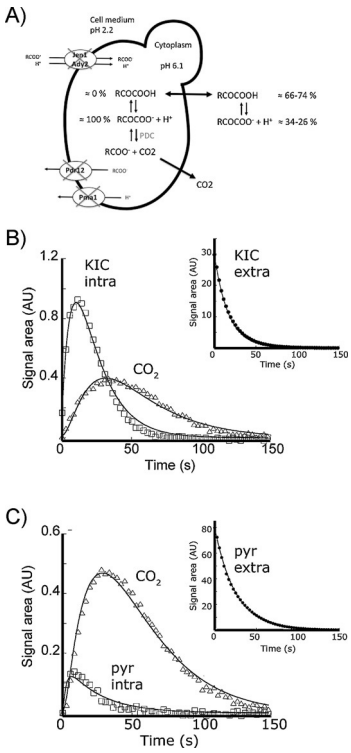

Figure 2. A) Experimental setup showing the uptake and conversion of the alpha-keto carboxylic acids at pH 2.2 in yeast cells as well as the loss of ^{13}C-label into CO_2 catalyzed by the yeast cytosolic enzyme pyruvate decarboxylase (PDC). B) Evolution of [1-^{13}C]ketoisocaproate (KIC) signal. Fitting of model to the intracellular signal, the subsequent production of CO_2, and the decaying extracellular signal (inset). C) Evolution of [1-^{13}C]pyruvate (pyr) signal. Fitting of model to the intracellular signal, the subsequent production of CO_2, and the decaying extracellular signal (inset). Signals in (B) and (C) were modeled using a three-pool model using the sum of three individual datasets for KIC (2 mM) and pyr (8 mM).

imately 9 s, significantly shorter than the measured value for the extracellular acetic acid, 40 ± 2 s.

In a variant of the yeast-cell experiment, a hyperpolarized α-keto carboxylic acid, either [1-^{13}C]keto-isocaproic acid (KIC) or [1-^{13}C]pyruvic acid, was supplied. In these experiments, the extracellular pH was lowered to 2.2 to ensure efficient uptake of these acids, which have pK_a values of 2.65 and 2.5, respectively (Figure 2 A). The reaction mechanisms of the alpha-keto acids are more complicated than that for acetate since these acids are metabolized in yeast cells by the enzyme pyruvate decarboxylase (PDC). Although pyruvate is the preferred substrate, this enzyme also acts on KIC. Decarboxylation results in the cleavage of the ^{13}C-label, which results in the formation of $^{13}CO_2$. Therefore, signals from the extracellular carboxylic acid and intracellular carboxylate forms and the metabolic product CO_2 were fitted to a three-pool model (Supporting Information, Section S3), resulting in values for the intracellular T_1 of [1-^{13}C]KIC and [1-^{13}C]pyruvate of 10.4 s and 12.7 s, respectively, (Figure 2 B,C). These values are 2.5–3-fold lower than the extracellular T_1 values.[8] The three-pool model also permits measurement of the T_1 for the product, CO_2. As a small uncharged molecule, CO_2 is exported by free diffusion through the cell membrane following a concentration gradient over an approximately 50-fold difference in volume from inside to outside the cells. The extracellular T_1 of CO_2 obtained in the yeast experiments (42 ± 6 s) corresponds well with an extracellular measured T_1 of 38 s and values in the literature.[9]

Two additional small carboxylic acids, lactic and butyric acid, which are commonly used as substrates in dDNP metabolic studies, were studied in the yeast system. The carboxylic acids were hyperpolarized and supplied at an extracellular pH of 2.2 for lactic acid (pK_a 3.86) and 4.2 for butyric acid (pK_a 4.82). Despite the low pH, at which all lactic acid is in the protonated form, no intracellular lactate was detected. In contrast, butyric acid diffused into the yeast cells with a rate more than 20-fold faster than that of acetic acid (Figure 3). At this high uptake rate, the intracellular concentration of butyrate would, if no re-export took place, amount to approximately 20 mM in 100 s. No acidification of the cytosol was detected during the experimental time window (160 s), which suggests that the yeast cells effectively control their pH by homeostasis. Instead, significant re-export of butyrate takes place even at very low extracellular substrate concentrations (0.17 mM) and results in the need for inclusion of an export term when modeling this data. The re-export introduced ambiguity in the data fitting, which was solved by measuring the extracellular T_1 in a separate experiment and using the resulting T_1 as an additional input in the model (Figure 3 B). An unambiguous determination of the intracellular T_1 of [1-^{13}C]butyrate (8.1 ± 0.6 s) could then be obtained.

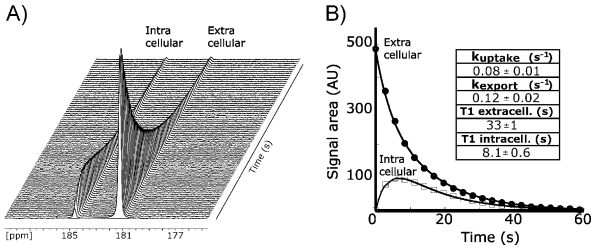

Figure 3. Butyrate uptake in yeast cells. A) Extracellular (181.2 ppm) and intracellular (184.7 ppm) signal evolution. B) Data fitting to the decaying extracellular butyric acid signal and the intracellular butyrate signal shown for one dataset (0.17 mM). Signals in (B) are modeled using a two-pool exchange model including three datasets (0.17 mM, $n=3$). The inset table lists measured average uptake rate, export rates, and T_1 relaxation constants.

The obtained uptake rates for acetate, butyrate, keto-isocaproate, and pyruvate correlate well with approximate experimental Log*P* values for the different acids (Table 1),

Table 1: Model-extracted import rates and experimental hydrophobicity (Log*P*) and pKa values for small carboxylic acids.

Carboxylic acid	Import rate [s^{-1}]	Log*P*[a]	pK_a[a]
Butyric acid	0.08 ± 0.01	0.79	4.82
Keto-isocaproic acid	0.008	n.a.	2.65
Acetic acid	0.004 ± 0.0005	−0.17	4.76
Pyruvic acid	0.0008	−0.5	2.50
Lactic acid	No import	−0.72	3.86

[a] Experimental values taken from www.drugbank.ca.

which suggests that the large differences in cross membrane diffusion rates are related to differences in lipophilicity. The uptake rate of pyruvic acid is low, and relatively high substrate concentrations were needed to measure the intracellular signal. That no signal from intracellular lactate could be detected may thus be ascribed to the relative hydrophilicity of this compound.

Macromolecular crowding, which reflects viscosity, solute binding, and/or collisional interactions, in the cytosol is a likely reason for the short intracellular T_1 values that were measured for the four small carboxylic acids.[10] A reduced apparent diffusion constant, reflecting the intracellular environment, has also been observed for lactate in vivo.[11] Very different protocols have been suggested in the literature to mimic macromolecular crowding in the cytosol.[12,13] We evaluated whether such an artificial cytosol (AC) could cause a shortening of the T_1 of small carboxylic acids and thus act as a prediction tool for intracellular T_1 values of other carboxylic acids. A mixture of ethanol, sucrose, and buffers efficiently lowered the T_1 of the investigated carboxylic acids (Supporting Information, Section S4). Although not a macromolecule, a high sucrose concentration imposes a similar restriction in mobility of the carboxylic acids by displacing water. Excellent correlation was obtained between the T_1 measured in the AC and the intracellular measured T_1 (Table 2). From a comparison between the T_1 measured in the AC and the intracellular measured T_1 values of hyperpolarized [1-^{13}C]acetate, [1-^{13}C]KIC, [1-^{13}C]pyruvate, and [1-^{13}C]butyrate, it may be expected that relative intracellular T_1 values can be used to predict the intracellular T_1 of carboxylic acids that cannot be easily obtained from a cellular model system (Table 2).

Table 2: The intracellular ($T_{1,int}$) relaxation rate constants are obtained from data fitting. $T_{1,AC}$ lists relaxation rates measured in an artificial cytosol. These are also given relative to acetate (relative $T_{1,AC}$) and used to predict T_1 values relative to the measured $T_{1,int}$ value for acetate (predicted $T_{1,int}$).

Carboxylic acid	$T_{1,int}$	$T_{1,AC}$	Relative $T_{1,AC}$	Predicted $T_{1,int}$
Butyric acid	8.1 ± 0.6	8.5	0.85	7.7
Keto-isocaproic acid	10.4	11	1.1	9.9
Acetic acid	9.0 ± 1.0	10	1.0	9.0
Pyruvic acid	12.7	15	1.5	13.5
Lactic acid	NA	5	0.5	4.5

In the literature in which kinetic fitting based on hyperpolarized NMR signals is used, it is a common assumption that the T_1 values for the intracellular and extracellular fractions of a compound are equal or similar.[14,15] The experiments described here do not support this assumption. This finding has major implications for the estimation of intracellular reaction rates. For example, assuming that the T_1 of acetate is the same inside and outside the cell results in an overestimation of the uptake rate by a factor four (Supporting Information, Section S5).

The data herein show the first measurements of intracellular T_1 values for small carboxylic acids, and the implications for quantitative analysis of hyperpolarized data are demonstrated.

Acknowledgements

We acknowledge the Danish National Research Foundation [grant DNRF124] for funding of this project.

Keywords: carboxylic acids · dissolution DNP · hyperpolarization · longitudinal relaxation · NMR spectroscopy

How to cite: *Angew. Chem. Int. Ed.* **2016**, *55*, 13567–13570
Angew. Chem. **2016**, *128*, 13765–13768

[1] T. W. M. Fan, A. N. Lane, *Prog. Nucl. Magn. Reson. Spectrosc.* **2016**, *92–93*, 18.
[2] M. J. Smith, C. B. Marshall, F.-X. Theillet, A. Binolfi, P. Selenko, M. Ikura, *Curr. Opin. Struct. Biol.* **2015**, *32*, 39.
[3] M. H. Lerche, P. R. Jensen, M. Karlsson, S. Meier, *Anal. Chem.* **2015**, *87*, 119.
[4] P. R. Jensen, M. Karlsson, M. H. Lerche, S. Meier, *Chem. Eur. J.* **2013**, *19*, 13288.
[5] M. Casal, O. Queirós, G. Talaia, D. Ribas, S. Paiva, *Adv. Exp. Med. Biol.* **2016**, *892*, 229.
[6] M. Casal, H. Cardoso, C. Leâo, *Microbiology* **1996**, *142*, 1385.
[7] F. Reineri, V. Daniele, E. Cavallari, S. Aime, *NMR Biomed.* **2016**, *29*, 1022.
[8] At pH 2.2, 37 °C, and 9.4 T. This discrepancy may be even larger since the T_1 of pyruvate and KIC are longer at neutral pH.

[9] J. A. Surface, *In Situ High Pressure and Temperature ^{13}C NMR for the Study of Carbonation Reactions of CO_2*, PhD Thesis, Washington University, **2013**.
[10] H. P. Kao, J. R. Abney, A. S. Verkman, *J. Cell Biol.* **1993**, *120*, 175.
[11] L. V. Søgaard, F. Schilling, M. A. Janich, M. I. Menzel, J.-H. Ardenkjær-Larsen, *NMR Biomed.* **2014**, *27*, 561.
[12] P. M. Gilmartin, *Molecular Plant Biology: A Practical Approach*, *Vol. 2*, Oxford University Press, New York, **2002**, p. 252.
[13] G. Martorell, M. Adrover, G. Kelly, P. A. Temussi, A. Pastore, *Proteins Struct. Funct. Bioinf.* **2011**, *79*, 1408.
[14] C. Harrison, C. Yang, A. Jindal, R. J. DeBerardinis, M. A. Hooshyar, M. Merritt, A. D. Sherry, C. R. Malloy, *NMR Biomed.* **2012**, *25*, 1286.
[15] C. J. Daniels, M. A. Mclean, R. F. Schulte, F. J. Robb, A. B. Gill, N. McGlashan, M. J. Graves, M. Schwaiger, D. J. Lomas, K. M. Brindle, F. A. Gallagher, *NMR Biomed.* **2016**, *29*, 387.

Received: August 3, 2016
Published online: September 26, 2016

